

DBSCAN of Multi-Slice Clustering for Third-Order Tensors

Dina Faneva Andriantsiory¹, Joseph Ben Geloun¹, and Mustapha Lebbah²

¹ LIPN, UMR CNRS 7030 , Sorbonne Paris Nord University, Villetaneuse, France

² DAVID Lab, University of Versailles, Université Paris-Saclay, Versailles, France

Abstract. Several methods for triclustering three-dimensional data require as hyperparameters the cluster size set or the number of clusters in each dimension. These methods raise an issue since, for real datasets, those inputs cannot be known without extreme cost. Recently introduced, the Multi-Slice Clustering (MSC) tackles this issue by using a threshold parameter to perform the data clustering. The MSC finds signal slices that lie in a lower dimensional subspace of 3rd-order rank-1 tensor datasets. The present work addresses an extension of this algorithm, namely the MSC-DBSCAN, that extracts several slice clusters that lie in different subspaces, when the 3rd-order dataset is a sum of $r \geq 1$ rank-1 tensors. Our algorithm uses the same input as the MSC algorithm and reduces to the same cluster solution for rank-1 tensor dataset.

1 Introduction

From an algebraic point of view, an n -way or n -th order tensor is an element of the tensor product of n vector spaces, each of which has its own coordinate system [14]. The tensor order indicates the number of dimensions of the array. As a data structure, consider m_1 individuals with m_2 features and collect the data for each individual-feature pair at m_3 different times. This is an example of a dataset structured in three dimensions, see figure 1. A convenient way to encode such data is given by a tensor of order 3. Multidimensional data of this kind arises in several contexts such as neuroscience [19], genomics data [3,17] and computer vision [16]. To learn this data without having a detailed understanding of it, we use unsupervised learning. Due to their increasing complexity, the mining of higher dimensional data naturally proceeds by identifying subspaces with specific features. Clustering is one of the most popular unsupervised machine learning methods for extracting relevant information such as structural similarity in data. It proceeds by the partitioning of a dataset into meaningful groups or clusters. The cluster can be defined as a collection of objects that are similar to each other and dissimilar or different from the objects in the other clusters. Thus, several computational methods for clustering multidimensional data, from matrices to higher order tensors, have been introduced in the literature, see for example the review [11]. For a detailed account of various available approaches closer to our present work, see [10,14,12,9,2,6,4].

The general structure of clustering algorithms requires, obviously, the data to be treated but also hyperparameters (inputs): the number of clusters or cluster sizes. These hyperparameters are not easy to set, and more to the point, especially difficult to set for real data. Moreover, their values influence the quality of the algorithm’s output. In [1], the authors provide a method that replaces the number of clusters with a measure of similarity within a cluster. This method is called Multi-Slice Clustering (MSC) and it performs on 3rd-order tensors. The strong point of the MSC algorithm guarantees the quality of the output clustering according to an input threshold parameter (strong similarity within a cluster and strong cluster separation). The MSC method performs well while possesses less constraints on hyperparameters. It provides a good grasp on the cluster quality, and remains competitive compared to other methods for biclustering and triclustering such as TFS [9], Tucker+ k -means, CP+ k -means [15].

There is however a limitation of the application domain of the MSC method. Indeed, the latter is designed to find one cluster within rank-1 tensor datasets. Such a condition is equally difficult to verify for real data. Therefore, it is essential to extend this method to higher rank tensor datasets to enable multiple cluster learning.

In this paper, we present an extension of the MSC algorithm. The new method, named MSC-DBSCAN, is able to identify many clusters within a tensor dataset decomposed as a sum of several rank-1 tensors. As the name suggests it, this is a combined method of the MSC and the so-called DBSCAN (Density-Based Spatial Clustering of Applications with Noise) [8]. We start with the MSC method which delivers a cluster, then this output goes to the next step of either validation or refinement by the DBSCAN method. The full procedure takes the same input threshold parameter of the MSC method. If the input data is a rank-1 tensor, then the output is identical to that of the MSC algorithm. For $k > 1$ rank-1 tensor data, the extension makes a major difference compared to the MSC alone. In the latter case, the last DBSCAN process will split the larger cluster in several distinct clusters. We experimentally demonstrate the performance of our proposed method.

The paper is organized as follows: in section 2, we list our notation and detail our model. Section 3 reviews the MSC algorithm and its limitations. Then, in section 4, we present the MSC-DBSCAN algorithm after having set up its theoretical approach. In section 5, we apply the new algorithm to synthetic and real datasets and compare its performances with the MSC algorithm.

2 Notation and model

2.1 Notation

In this paper, we use $\mathcal{T}, \mathcal{X}, \mathcal{Z}$ to represent the dataset tensor, signal tensor, and noise tensor respectively. The matrices are represented by the capital letters A, C, T, V, Z . We use the Matlab notation for the entries of the tensor. $\|M\|$ and

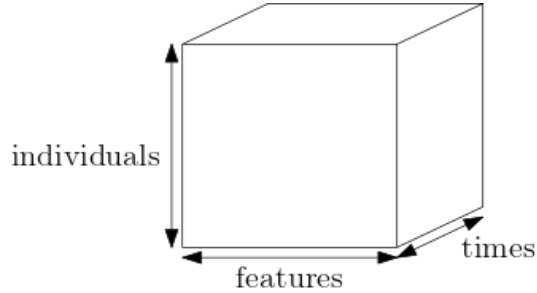


Fig. 1: The 3-order tensor dataset.

$\|M\|_F$ represent the operator norm and the Frobenius norm of the matrix M , respectively. For any matrix, A and $B = |A|$, the entries of B are the absolute value of the entries of A . The lowercase boldface letters $\mathbf{x}, \mathbf{v}, \mathbf{w}, \dots$ represent vectors and $\|\mathbf{x}\|_2$ is the euclidean norm of the vector \mathbf{x} , the lowercase $x, y, \alpha, \gamma, \lambda$ represent scalars. For any set J , $|J|$ denotes the cardinality of J and \bar{J} denotes the complementary of J in a larger set. For an integer $n > 0$, we denote $[n] = \{1, \dots, n\}$. The asymptotic notation $a(n) = \mathcal{O}(b(n))$ (res. $a(n) = \Omega(b(n))$) means that, there exists a universal constant c such that for sufficiently large n , we have $|a(n)| \leq cb(n)$ (resp. $|a(n)| \geq cb(n)$).

2.2 Model

We will be mainly interested in 3rd-order tensors. Thus, let $\mathcal{T} \in \mathbb{R}^{m_1 \times m_2 \times m_3}$ be our tensor dataset. We decompose it as $\mathcal{T} = \mathcal{X} + \mathcal{Z}$, where \mathcal{X} is called the signal tensor and \mathcal{Z} the noise tensor.

A CANDECOMP/PARAFAC (CP) decomposition of a tensor defines it as a sum of r rank-1 tensors [14]. Assuming a particular CP-decomposition of the signal tensor, we write:

$$\mathcal{T} = \mathcal{X} + \mathcal{Z} = \sum_{i=1}^r \gamma_i \mathbf{w}_i \otimes \mathbf{u}_i \otimes \mathbf{v}_i + \mathcal{Z} \tag{1}$$

where $\forall i, \gamma_i > 0$ stands for the signal strength, $\mathbf{w}_i \in \mathbb{R}^{m_1}$, $\mathbf{u}_i \in \mathbb{R}^{m_2}$ and $\mathbf{v}_i \in \mathbb{R}^{m_3}$ are unit vectors, and for a fix i_0 , $\mathbf{w}_{i_0} \otimes \mathbf{u}_{i_0} \otimes \mathbf{v}_{i_0}$ is called a rank-1 tensor [14].

Each low-dimensional subspace or rank-1 tensor corresponds to one cluster. The cluster sets from mode-1, mode-2, and mode-3 in the i -th subspace are denoted by J_1^i, J_2^i , and J_3^i . Concerning the noise model, we assume that the entries of \mathcal{Z} are independently identically distributed (i.i.d) and have a standard normal distribution. This is the traditional noise model in an unsupervised learning method for tensor data, see for instance [9,5].

For a fixed i (a cluster index), the Cartesian product of a pair of sets from J_1^i, J_2^i , and J_3^i represents the tensor biclustering. The collection of the three sets defines a triclustering [9,18].

3 Multi-Slice Clustering for 3-order tensor: a review

In this section, we provide a lightening review of [1].

Equation (1) with $r = 1$ describes our tensor modeling. This means that the signal tensor is of the form $\mathcal{X} = \gamma \mathbf{w} \otimes \mathbf{u} \otimes \mathbf{v}$. Fixing one index of \mathcal{T} and collecting the set of data entries defines a matrix or slice of the tensor. The MSC method aims at finding, in each dimension of the tensor \mathcal{T} , the indices of the matrix slices that are highly similar up to a threshold parameter ϵ . The output of the MSC algorithm is therefore a single 3D cluster.

Fixing an index i in the mode-1 of \mathcal{T} , we obtain a matrix $T_i \in \mathbb{R}^{m_2 \times m_3}$ defined by (Matlab notation)

$$T_i = \mathcal{T}(i, :, :) = \mathcal{X}(i, :, :) + \mathcal{Z}(i, :, :) = X_i + Z_i \quad (2)$$

The slice T_i is a sum of the corresponding slice from the signal tensor X_i and the noise tensor Z_i . A similar principle is applied to mode-2 or mode-3 of the tensor to collect slices in the remaining modes.

The MSC learns the information within each slice via spectral analysis. To do so, it starts with the computation of the slice covariance matrix $C_i = T_i^t T_i$. The largest eigenvalue and corresponding eigenvector associated with the matrix C_i , covers the most relevant information in each slice indexed by i .

Our task is the determination of the element of J_1 in mode-1. Recovering J_2 and J_3 in the rest of the modes follows the same idea. For all slices, we denote by $\underline{\lambda}_i$ the top eigenvalue and $\tilde{\mathbf{v}}_i$ the top eigenvector of C_i for $i \in [m_1]$. The following matrix contains the dispersion of information of all slices

$$V = [\tilde{\lambda}_1 \tilde{\mathbf{v}}_1 \cdots \tilde{\lambda}_{m_1} \tilde{\mathbf{v}}_{m_1}] \quad (3)$$

where we set $\tilde{\lambda}_i$ to $\underline{\lambda}_i/\lambda, \forall i \in [m_1]$, and $\lambda = \max(\underline{\lambda}_1, \dots, \underline{\lambda}_{m_1})$. We construct the matrix C defined as $C = |V^t V|$ that now contains the similarity between slices. The marginal sum of each row of C is $d_i, i \in [m_1]$. These form a vector \mathbf{d} of marginal sums. The selection of the cluster J_1 uses the vector \mathbf{d} , and the following theorem guarantees the quality within the output cluster (see theorem III.1 in [1]).

Theorem 1. *Let $l = |J_1|$, assume that $\sqrt{\epsilon} \leq \frac{1}{m_1 - l}$. $\forall i, n \in J_1$, for $\lambda = \Omega(\mu)$, there is a constant $c_1 > 0$ such that*

$$|d_i - d_n| \leq l \frac{\epsilon}{2} + \sqrt{\log(m_1 - l)} \quad (4)$$

holds with probability at least $1 - e(m_1 - l)^{-c_1}$, where $\mu = (\sqrt{m_2 - 1} + \sqrt{m_3})^2$.

The assumption of a rank-1 tensor is viewed as a principal limitation of the application of the MSC method. In this section, we propose a radical improvement and extension of the MSC algorithm to determine more clusters from the input dataset. Therefore, we assume that the dataset is approximated by a sum of r rank-1 tensors (with $r \geq 1$). To illustrate our method, we focus on $r = 2$ but our explanations will easily stand for $r \geq 2$. The following statement proves that the MSC is insufficient for detecting multiple triclusters.

Proposition 1. *Let J_1 and J_2 be two disjoint slice clusters that lie in two different subspaces. By simplicity, we assume that $\lambda \approx \lambda_{(1)} \approx \lambda_{(2)} = \Omega(m_1)$ and $|J_1| = |J_2| = l$, then the MSC gathers the two clusters as one cluster of slices with high probability.*

Proof. This is a corollary of theorem 1. We expand the difference $|d_i - d_j|$, with $i \in J_1$ and $j \in J_2$ into sums of similarity entries that belong to $J_1 \cup J_2$ or not. Each term will be bounded using theorem 1.

Two other theorems in [1] show the proper separation of the cluster and the rest of the data, proving also that the MSC performs well for $r = 1$. Our interest lies in $r > 1$ and will motivate our next study.

4 MSC-DBSCAN

In this section, without loss of generality, we assume that our dataset is a sum of 2 rank-1 tensors. The generalization of the method to a general tensor follows the same idea.

4.1 Problem formulation

Let $\mathcal{T} \in \mathbb{R}^{m_1 \times m_2 \times m_3}$ be the tensor dataset. It decomposes as $\mathcal{T} = \mathcal{X} + \mathcal{Z}$ where \mathcal{X} is the signal tensor and \mathcal{Z} is the noise tensor. We assume that

$$\mathcal{T} = \mathcal{X} + \mathcal{Z} = \sum_{i=1}^r \gamma_i \mathbf{w}_i \otimes \mathbf{u}_i \otimes \mathbf{v}_i + \mathcal{Z} \quad (5)$$

where $\forall i, \gamma_i > 0$ stands for the signal strength, $\mathbf{w}_i \in \mathbb{R}^{m_1}$, $\mathbf{u}_i \in \mathbb{R}^{m_2}$ and $\mathbf{v}_i \in \mathbb{R}^{m_3}$ are unit vectors. Thus, the signal \mathcal{X} is a sum of r rank-1 tensors.

The MSC method selects the elements of the cluster from the marginal similarity vector \mathbf{d} of each slice. However, for a dataset with CP-decomposition as a sum of more than one rank-1 tensors, two slices of indices i and j ($i \neq j$) which have similarity close to zero may have the same corresponding entries in the vector \mathbf{d} . If the tensor dataset is decomposed as the sum of several rank-1 tensors, the inequality of theorem 1 may fail for the determination of a single cluster. Thus, there is room for having several clusters within the detected MSC cluster.

We illustrate the occurrence of two clusters in the following:

- If the two clusters are well separated, there is a gap between the marginal similarity values within the vector \mathbf{d} . See figure 3b. This case may happen in two situations: (1) the two clusters have same size, and the top eigenvalues corresponding to the two clusters have a significant difference; (2) the two clusters have the same eigenvalue but the cluster sizes are very different ($|J_2| \gg |J_1|$). In this case, we can run iteratively the MSC method to detect J_1 and J_2 . Indeed, running first MSC detects the elements of J_1 and, then running again the MSC on the remaining dataset will enable to detect the second cluster J_2 (we can keep up on the rest of the data).

- If there is no significant gap between the two clusters, the MSC method gathers the two clusters in one which is then output. This is because the necessary condition of the equation (4) in theorem 1 is verified for all elements in $J_1 \cup J_2$. We illustrate this case in figure 3a. This case happens when: (1) the top eigenvalues associated with the covariance matrices of the cluster slices are equal and the two cluster sets have the same cardinality; (2) another possibility is when there are similar entries (corresponding to two or more slices) within the vector \mathbf{d} . In this case, an iteration of the MSC method will not separate the elements of the clusters. The proof of this statement is presented in proposition 1.

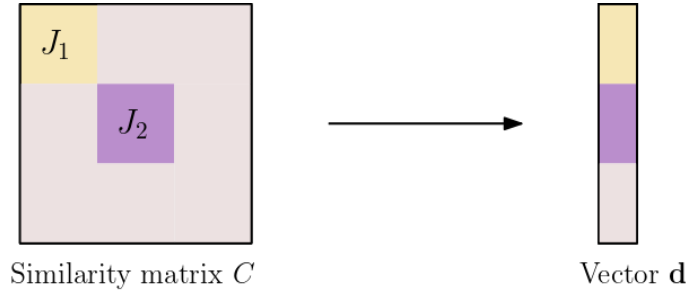


Fig. 2: Similarity matrix C for a tensor with two disjoint clusters and the corresponding vector \mathbf{d} .

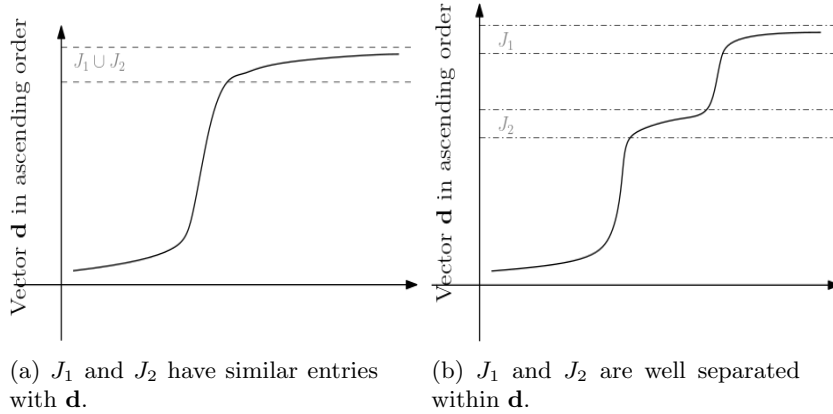


Fig. 3: Plot of the entries of the vector \mathbf{d} in ascending order.

We propose the MSC-DBSCAN method to solve this problem and to distinguish these clusters.

4.2 MSC-DBSCAN method

As its name suggests it, the MSC-DBSCAN method is a sequence of two methods. It starts with the MSC, then it follows a verification/validation/refinement

of the cluster output with the DBSCAN analysis (Density-Based Spatial Clustering of Applications with Noise) [8]. The MSC method, based on the hyperparameter ϵ , first delivers 3 slice clusters, one for each mode. As a second move, the DBSCAN analysis refines the similarity relation between the slices of the selected cluster. If the output is exactly one cluster (cannot be further clustered), then the MSC-DBSCAN will confirm it. However, if the output of the MSC may be further decomposed in different clusters, the DBSCAN will proceed with the splitting of the initial output result. We must keep in mind that the DBSCAN needs two hyperparameters to detect the cluster in the input: the neighborhood radius and the minimal number of neighborhoods, denoted by ϵ and $Minpts$, respectively. Thus, one realizes that the second part of the procedure has all necessary information withdrawn the MSC method.

The hyperparameter ϵ is obtained from the hyperparameter of the MSC algorithm ϵ , and the cluster size of the output l . The neighborhood radius is

$$\epsilon = \sqrt{\frac{l\epsilon}{2} + \sqrt{\log(m_1 - l)}} \quad (6)$$

and we take the minimum neighborhoods as $Minpts = 2$. We use the euclidean distance to measure the dissimilarity in the splitting algorithm. The following theorem justifies the performance of the method.

Theorem 2. *We denote by J the output clustering output from the MSC algorithm. Let J_1 and J_2 the two disjoint clusters lie in two different subspaces such that $J = J_1 \cup J_2$. Then,*

– for $i, j \in J_1$ (or belonging to J_2), we have

$$d(c_i., c_j.) \leq \sqrt{\frac{l\epsilon}{2} + \sqrt{\log(m_1 - l)}}, \quad (7)$$

– for $i \in J_1$ and $j \in J_2$, we have,

$$d(c_i., c_j.) \geq \sqrt{\frac{l\epsilon}{2} + \sqrt{\log(m_1 - l)}}. \quad (8)$$

with a high probability when m_1 becoming large, where $c_i.$ represents the i -th column of matrix C .

Proof. By definition of the vector \mathbf{d} and $i, j \in J_1$ and $|J_1|=l$, we have

$$\begin{aligned} d(c_i., c_j.)^2 &= \sum_{k \in [m_1]} (c_{ik} - c_{jk})^2 \leq \sum_{k \in [m_1]} |c_{ik} - c_{jk}| \\ &\leq \sum_{k \in J_1} |c_{ik} - c_{jk}| + \sum_{k \in \bar{J}_1} |c_{ik} - c_{jk}| \\ &\leq \frac{l\epsilon}{2} + \sqrt{\log(m_1 - l)}. \end{aligned}$$

We have the first inequality because $-1 \leq c_{ik} - c_{jk} \leq 1$ for all $k \in [m_1]$. The last inequality is held if by the clustering condition of the MSC method (theorems 1 and theorem III.2 of [1]).

For $i \in J_1, j \in J_2$, with the hypothesis $\mathbf{v}_i \perp \mathbf{v}_j$ by the definition of the rank decomposition and $|J_1| = |J_2| = l$, we have

$$\begin{aligned}
d(c_i, c_j)^2 &= \sum_{k \in [m_1]} (c_{ik} - c_{jk})^2 \\
&= \sum_{k \in [m_1]} c_{ik}^2 + c_{jk}^2 - 2c_{ik}c_{jk} \\
&\geq \sum_{k \in J_1} (c_{ik}^2 + c_{jk}^2 - 2c_{ik}c_{jk}) + \sum_{k \in J_2} (c_{ik}^2 + c_{jk}^2 - 2c_{ik}c_{jk}) \\
&\quad + \sum_{k \in [m_1] \setminus (J_1 \cup J_2)} (c_{ik} - c_{jk})^2
\end{aligned} \tag{9}$$

According to the hypothesis $\mathbf{v}_i \perp \mathbf{v}_j$, for $j \in J_2$ and $k \in J_1$ we have $c_{jk} = 0$. In the same vein, for $i \in J_1$ and $k \in J_2$, we have $c_{ik} = 0$. Using the ϵ -similarity ([1], definition III.2), the equation (9) becomes:

$$d(c_i, c_j)^2 \geq \sum_{k \in J_1} c_{ik}^2 + \sum_{k \in J_2} c_{jk}^2 \geq 2l^2(1 - \frac{\epsilon}{2})^2 \tag{10}$$

Hence,

$$d(c_i, c_j) \geq \sqrt{2}l(1 - \frac{\epsilon}{2}) \geq \sqrt{\frac{l\epsilon}{2} + \log(m_1 - l)} \tag{11}$$

which is the claim.

The detailed steps of our method is shown in algorithm 1. In this algorithm, the upper-script $j \in \{1, 2, 3\}$, appearing for instance in $J^{(j)}$, represents the studied mode of the tensor. The under-script i of $J_i^{(j)}$ identifies the different clusters in the corresponding mode j .

5 Experiments

To evaluate the performance of the present clustering method, we first use two indices suitable for synthetic data. First, we discuss the ARI [13], and then the cluster quality with respect to the similarity will tested through the root mean square error (RMSE) [7]. We start the experiments with the synthetical data, and then we process a real dataset.

Synthetical results – Here, we generate a synthetic dataset as a sum of 2 rank-1 tensors plus the noise tensor. We run the MSC and MSC-DBSCAN algorithms on our data, detect the different clusters, and compare their quality.

Algorithm 1 MSC-DBSCAN

Require: 3rd-order tensor $\mathcal{T} \in \mathbb{R}^{m_1 \times m_2 \times m_3}$, threshold parameter ϵ
Ensure: $(J_i^{(1)}, J_i^{(2)}, J_i^{(3)})_i$

- 1: **for** j in $\{1, 2, 3\}$ **do**
- 2: Initialize the matrix M
- 3: Initialize $\lambda_0 \leftarrow 0$
- 4: **for** i in $\{1, 2, \dots, m_j\}$ **do**
- 5: Compute : $C_i \leftarrow T_i^t T_i$
- 6: Compute the spectral decomposition of C_i
- 7: Compute $M(:, i) \leftarrow \lambda_i * \mathbf{v}_i$
- 8: **if** $\lambda_i > \lambda_0$ **then**
- 9: $\lambda_0 \leftarrow \lambda_i$
- 10: **end if**
- 11: **end for**
- 12: Compute : $V \leftarrow M / \lambda_0$
- 13: Compute : $C \leftarrow |V^t V|$
- 14: Compute : \mathbf{d} the vector marginal sum of C and sort it
- 15: Initialization of $J^{(j)}$ using the maximum gap in \mathbf{d} sorted
- 16: Compute : $l \leftarrow |J^{(j)}|$
- 17: **while** not convergence of the elements of $J^{(j)}$ (theorem 1) **do**
- 18: Update the element of $J^{(j)}$ (excluding i s.t. d_i is the smallest value that violates theorem 1)
- 19: Compute l
- 20: **end while**
- 21: Build the similarity of all indices in $J^{(j)}$ from the matrix C
- 22: Apply DBSCAN algorithm with hyper-parameter $\epsilon = \sqrt{\frac{l\epsilon}{2}} + \sqrt{\log(m_1 - l)}$ and $Minpts = 2$ in order to get the set $(J_i^{(j)})_i$.
- 23: **end for**

The data is built as in equation (5). We consider a tensor with $r = 2$ rank-1 tensors. Each factor matrix contains 2 columns vectors which are orthogonal. Since the MSC cluster selection is independent in each mode, the following explanation focuses only on the first mode of the tensor. The same operations in the remaining modes are easily implemented and analogous.

We generate tensor datasets with $m_1 = m_2 = m_3 = 50$, and introduce two clusters lying in two different subspaces within the data. In mode-1, the two cluster sets of the slices are denoted by J_1 and J_2 ; they obey $J_1 \cap J_2 = \emptyset$. Based on the similarity measure, the elements of J_1 are highly dissimilar to the elements of J_2 . The two clusters have the same cardinality $|J_1| = |J_2| = 10$. The signal tensor is constructed as the following way:

$$\begin{aligned}
 \mathbf{u}_1(i) &= \begin{cases} \frac{1}{\sqrt{|J_1|}} & \text{if } i \in J_1, \\ 0 & \text{otherwise} \end{cases} \\
 \mathbf{u}_2(i) &= \begin{cases} \frac{1}{\sqrt{|J_2|}} & \text{if } i \in J_2, \\ 0 & \text{otherwise} \end{cases}
 \end{aligned} \tag{12}$$

The same cluster construction of equation (12) extends to mode-2 and mode-3 of the tensor. The entries of the tensor noise are standard Gaussian random variable independent and identically distributed.

First, we evaluate the performance of the MSC-DBSCAN by varying the signal strength value γ_i , $i = 1, 2$, for the rank-1 tensors. We assume that the 2 rank-1 tensors have the same weight $\gamma_i = \gamma$ and let γ vary from 50 to 100. We run the algorithm 10 times for each value of γ . The two cluster sets of each mode have the same cardinality. The value of the ϵ is chosen to be 0.001 during the experiment in order to satisfy the hypothesis of the main MSC theorem. For each iteration, we rate the quality of the output by computing its ARI. The results are displayed in figure 4.

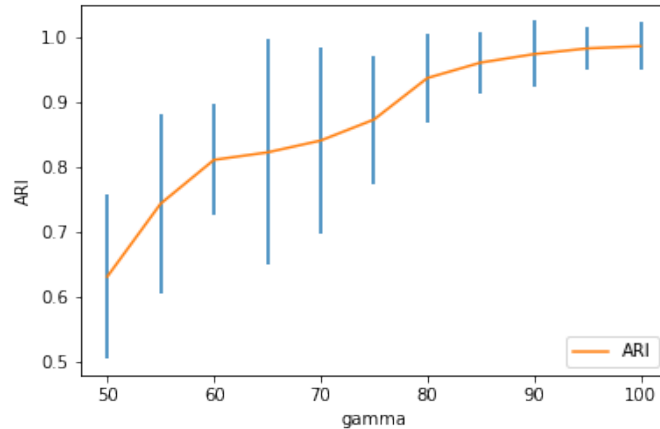


Fig. 4: The ARI of the output of MSC-DBSCAN for γ ranges from 50 to 100.

The curve in figure 4 represents the mean and the vertical blue line represents the standard deviation of the ARI for the 10 experiments. As a result, the ARI increases and tends to 1 as the value of γ becomes higher. It is stable and very close to the maximum at $\gamma = 80$. This shows that the MSC-DBSCAN performs well and is able to recover the 2 clusters for increasing values of the signal strength.

Secondly, on the same synthetic data, we compare the quality of the MSC and MSC-DBSCAN algorithms with the same value of the hyperparameter ϵ . We set the value of γ to 80. We run the experiment 20 times and regenerate the data for each iteration. The RMSE serves as an evaluation of the clustering performance. This error is computed in the sub-cube (triclustering) generated by the combination of the clusters of the 3 modes.

Figure 5 shows that the RMSE of the sub-cube given with the MSC algorithm is very high compared to the RMSE of the sub-tensors delivered by the MSC-DBSCAN algorithm. The reason of this difference has the following explanation. There are 2 well-separated clusters in each mode. The MSC algorithm combines the elements of these two clusters into one cluster because they have almost the same value within the vector \mathbf{d} . On the other hand, the MSC-DBSCAN has

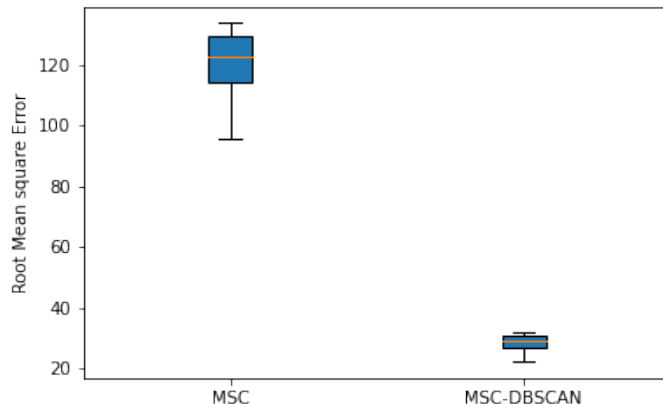


Fig. 5: Represents the root mean square error of the sub-cube(s) generated from the output of MSC and MSC-DBSCAN algorithms.

split the output of the MSC method into two clusters. This obviously reduces the RMSE (clusters of smaller size generate high similarity). The MSC-DBSCAN method enhances the clustering quality in the case of multiple clusters.

Although, we have not presented the results here, we note the following fact: if the clusters are well separated (a significant difference is noticed in the vector marginal sum \mathbf{d}), then the outputs of the MSC and the MSC-DBSCAN are the same.

Real data: preliminary results – We run the MSC-DBSCAN on the same real data [1] set used in the MSC. The output of the MSC-DBSCAN delivers only one cluster lying in one subspace. This cluster is identical to the output of the MSC algorithm. Therefore, this confirms that such real dataset contains only a single cluster. Due to the lack of real datasets, we have not perform other experiments on the present algorithm. This must be done in the future.

The MSC-DBSCAN code is available at this link:
<https://github.com/ANDRIANTSIORY/MSC-DBSCAN>.

6 Conclusion

The MSC method and performance rest on a particular type of input: a rank-1 tensor. If the tensor can be decomposed as a sum of a rank-1 tensors, the MSC algorithm is of limited efficiency and even relevance. This situation may very well occur for real dataset. We have proposed an extension and improvement of the MSC method able to address that generic situation: the MSC-DBSCAN. The MSC-DBSCAN provides the same output cluster as MSC for a rank-1 tensor. In addition, it is able to extract several clusters in 3rd-order datasets, sum of rank-1

tensors. Statistical theorems ensure the method reliability. We have performed conclusive experimental tests and shown the effectiveness of the new algorithm compared to MSC method.

References

1. Andriantsiory, D.F., Ben Geloun, J., Lebbah, M.: Multi-slice clustering for 3-order tensor. In: 2021 20th IEEE International Conference on Machine Learning and Applications (ICMLA). pp. 173–178. IEEE (2021)
2. Andriantsiory, D.F., Lebbah, M., Azzag, H., Beck, G.: Algorithms for an efficient tensor biclustering. U. L., Lauw H. (eds) Trends and Applications in Knowledge Discovery and Data Mining. PAKDD 2019 **11607** (2019)
3. Ardlie, K., DeLuca, D., Segrè, A., Sullivan, T., Young, T., Gelfand, E., Trowbridge, C., Maller, J., Tukiainen, T., Lek, M., Ward, L., Kheradpour, P., Iriarte, B., Meng, Y., Palmer, C., Esko, T., Winckler, W., Hirschhorn, J., Kellis, M., Lockhart, N.: The genotype-tissue expression (gtex) pilot analysis: Multitissue gene regulation in humans. *Science* **348**(6235), 648–660 (2015)
4. Bach, F., Jordan, M.: Learning spectral clustering. *Advances in neural information processing systems* **16**(2), 305–312 (2004)
5. Cai, T.T., Liang, T., Rakhlin, A.: Computational and statistical boundaries for submatrix localization in a large noisy matrix. *The Annals of Statistics* **45**(4), 1403–1430 (2017). <https://doi.org/10.1214/16-aos1488>
6. Carson, T., Mixon, D.G., Villar, S.: Manifold optimization for k-means clustering. In: 2017 International Conference on Sampling Theory and Applications (SampTA). pp. 73–77 (2017). <https://doi.org/10.1109/SAMPSTA.2017.8024388>
7. Chai, T., Draxler, R.R.: Root mean square error (rmse) or mean absolute error (mae)?—arguments against avoiding rmse in the literature. *Geoscientific model development* **7**(3), 1247–1250 (2014)
8. Ester, M., Kriegel, H.P., Sander, J., Xu, X., et al.: A density-based algorithm for discovering clusters in large spatial databases with noise. In: *kdd*. vol. 96, pp. 226–231 (1996)
9. Feizi, S., Javadi, H., Tse, D.: Tensor biclustering. In: Guyon, I., Luxburg, U.V., Bengio, S., Wallach, H., Fergus, R., Vishwanathan, S., Garnett, R. (eds.) *Advances in Neural Information Processing Systems*. vol. 30, pp. 1311–1320 (2017)
10. Friedlander, M.P., Hatz, K.: Computing non-negative tensor factorizations. *Optimization Methods and Software* **23**(4), 631–647 (2008). <https://doi.org/10.1080/10556780801996244>, <https://doi.org/10.1080/10556780801996244>
11. Henriques, R., Madeira, S.C.: Triclustering algorithms for three-dimensional data analysis: A comprehensive survey. *ACM Computing Surveys (CSUR)* **51**(5), 1–43 (2018). <https://doi.org/10.1145/3195833>
12. Hore, V., Viñuela, A., Buil, A., Knight, J., McCarthy, M.I., Small, K., Marchini, J.: Tensor decomposition for multiple-tissue gene expression experiments. *Nature genetics* **48**(9), 1094–1100 (2016)
13. Hubert, L., Arabie, P.: Comparing partitions. *Journal of Classification* **2**(1), 193–218 (1985). <https://doi.org/10.1007/BF01908075>
14. Kolda, T.G., Bader, B.W.: Tensor decompositions and applications. *SIAM review* **51**(3), 455–500 (2009). <https://doi.org/10.1137/07070111X>, <https://doi.org/10.1137/07070111X>

15. Sun, W.W., Li, L.: Dynamic tensor clustering. *Journal of the American Statistical Association* **114**(528), 1894–1907 (2019). <https://doi.org/10.1080/01621459.2018.1527701>, <https://doi.org/10.1080/01621459.2018.1527701>
16. Tang, Y., Salakhutdinov, R., Hinton, G.: Tensor analyzers. In: Dasgupta, S., McAllester, D. (eds.) *Proceedings of the 30th International Conference on Machine Learning*. *Proceedings of Machine Learning Research*, vol. 28, pp. 163–171 (2013), <https://proceedings.mlr.press/v28/tang13.html>
17. Wang, M., Fischer, J., Song, Y.: Three-way clustering of multi-tissue multi-individual gene expression data using semi-nonnegative tensor decomposition. *The Annals of Applied Statistics* **13**(2), 1103–1127 (2019). <https://doi.org/10.1214/18-AOAS1228>
18. Zhao, L., Zaki, M.J.: Tricuster: an effective algorithm for mining coherent clusters in 3d microarray data. In: *Proceedings of the 2005 ACM SIGMOD international conference on Management of data*. pp. 694–705 (2005)
19. Zhou, H., Li, L., Zhu, H.: Tensor regression with applications in neuroimaging data analysis. *Journal of the American Statistical Association* **108**(502), 540–552 (2013). <https://doi.org/10.1080/01621459.2013.776499>, PMID: 24791032